Full length article

A chondrogenesis induction system based on a functionalized hyaluronic acid hydrogel sequentially promoting hMSC proliferation, condensation, differentiation, and matrix deposition

Binhong Teng[a], Siqi Zhang[b], Jijia Pan[b], Ziqian Zeng[a], Yang Chen[b], Yu Hei[b], Xiaoming Fu[a], Qian Li[b], Ming Ma[c], Yi Sui[a], Shicheng Wei[a,b,*]

[a] Department of Oral and Maxillofacial Surgery/Central Laboratory, School and Hospital of Stomatology, Peking University, Beijing 100081, PR China
[b] Laboratory of Biomaterials and Regenerative Medicine, Academy for Advanced Interdisciplinary Studies, Peking University, Beijing 100871, PR China
[c] Department of Oral Pathology, School and Hospital of Stomatology, Peking University, Beijing 100081, China

A B S T R A C T

Hydrogel scaffolds are widely used in cartilage tissue engineering as a natural stem cell niche. In particular, hydrogels based on multiple biological signals can guide behaviors of mesenchymal stem cells (MSCs) during neo-chondrogenesis. In the first phase of this study, we showed that functionalized hydrogels with grafted arginine-glycine-aspartate (RGD) peptides and lower degree of crosslinking can promote the proliferation of human mesenchymal stem cells (hMSCs) and upregulate the expression of cell receptor proteins. Moreover, grafted RGD and histidine-alanine-valine (HAV) peptides in hydrogel scaffolds can regulate the adhesion of the intercellular at an early stage. In the second phase, we confirmed that simultaneous use of HAV and RGD peptides led to greater chondrogenic differentiation compared to the blank control and single-peptide groups. Furthermore, the controlled release of kartogenin (KGN) can better facilitate cell chondrogenesis compared to other groups. Interestingly, with longer culture time, cell condensation was clearly observed in the groups with RGD and HAV peptide. In all groups with RGD peptide, significant matrix deposition was observed, accompanied by glycosaminoglycan (GAG) and collagen (Coll) production. Through *in vitro* and *in vivo* experiments, this study confirmed that our hydrogel system can sequentially promote the proliferation, adhesion, condensation, chondrogenic differentiation of hMSCs, by mimicking the cell microenvironment during neo-chondrogenesis.

Statement of significance

Using MSCs to repair and regenerate cartilage defects still faces many difficulties and challenges. Injectable hydrogel scaffolds provide a living environment for MSCs, but it is far removed from the native extracellular matrix. In particular, during the differentiation of stem cells into chondrocytes, cell behaviors, such as spontaneous proliferation, condensation, and differentiation, and matrix precipitation remain limited in hydrogel matrix. In this study, to make hydrogel matrix regulate these cell behaviors, we efficiently integrated biomimetic peptides and KGN into the hydrogel system. Through the respective roles of various peptides and the sustained release of KGN, this functionalized HA hydrogel has promise as a stem cell culture system and scaffold matrix for clinical applications.

© 2021 Acta Materialia Inc. Published by Elsevier Ltd. All rights reserved.

1. Introduction

Cartilage tissue, including knee, temporomandibular joint condylar cartilage, is vulnerable to trauma, tumors, infection, diseases, but is an indispensable component of human tissue [1,2].

* Corresponding author at: Department of Oral and Maxillofacial Surgery/Central Laboratory, School and Hospital of Stomatology, Peking University, Beijing 100081, PR China.
E-mail address: sc-wei@pku.edu.cn (S. Wei).

Due to the avascularity and low cellularity of cartilage, its ability to self-heal is very limited, which makes clinical treatment thereof highly challenging [3,4]. Tissue engineering based on synthetic hydrogels provides a solution to these well-documented problems [5,6]. Hyaluronic acid (HA) [7], sodium alginate [8], chitosan [9] and other natural materials have been used in fabrication of hydrogels. Each of these materials has its own advantages and disadvantages, such that they should be selected according to the specific research objectives. HA, is often used as a scaffold material for cartilage repair and regeneration, and constitutes an important component of the extracellular matrix (ECM) in cartilage, synovial fluid, and various tissues [10,11]. HA hydrogel matrix can facilitate survival and growth of the cells through providing three-dimensional (3D) environment, while the native ECM affects cells through complex constituents and dynamic 3D structures [12]. The capacity related to neochondrogenesis, such as cell proliferation, aggregation, differentiation and matrix deposition, remains limited in hydrogel matrix, especially for stable covalent cross-linked hydrogels. [13,14].

Mesenchymal stem cells (MSCs) show proliferation, cell-cell contact, and condensation, which precede chondrogenic differentiation and secretion of cartilage matrix [15]. To simulate the MSC microenvironment, biomimetic peptides are widely used to promote cellular activity in hydrogels. Arginine-glycine-aspartate (RGD) peptides, which are integrin binding ligands, can bond cells to ECM and initiate cell-related signaling events [16,17]. Previous reports have shown that RGD can promote cell spreading and proliferation in hydrogel systems [18,19]. In addition, the capacity of RGD peptides to regulate cell signaling behavior is closely related to the mechanical properties, degree of crosslinking, relaxation strain, etc., of the matrix [20,21]. Bian et al. found that MeHA with a higher degree of crosslinking promoted hypertrophic differentiation of stem cells and matrix calcification. High crosslinking intensity with matrix calcification also limits the secretion of cartilage stroma [22]. Chaudhari et al. found that changing the mechanical properties and relaxation modulus of gels can affect ligand clustering, the spreading and proliferation of cells, osteogenic differentiation, and ECM deposition [21]. Moreover, in a study on the effects of the physical properties of HA gel on chondrocytes, it was found that elastic stress regulated the production and apoptosis of chondrocytes [23]. These results suggest that for optimal mesenchymal chondrogenic differentiation, the effects of the stiffness of the hydrogel matrix on cells should be taken into account.

The interaction and agglutination of MSCs are necessary for cartilage formation. Cell-cell interactions can trigger high neural cadherin (N-cadherin) and neural cell adhesion molecule (NCAM) expression during adhesion, thus facilitating chondrogenic differentiation [24,25]. As a transmembrane protein, a histidine-alanine-valine (HAV) sequence derived from cadherin regulates cell–cell interactions [26]. Previous research suggests that grafting HAV peptides onto 3D electrospinning scaffolds promotes the aggregation of MSCs and upregulates the expression of NCAM, N-cadherin, and cartilage-related genes [15]. The addition of HAV peptides to hydrogel systems has been shown to facilitate chondrogenic differentiation in previous studies [27]. Although HAV is a good regulator of chondrogenic differentiation in MSCs, few studies have investigated its function on mesenchymal condensation in 3D hydrogel matrices [14,28]. To accurately reproduce the cartilage regeneration environment, cell aggregation in biomimetic matrix of hydrogels is necessary at an early stage.

The effects of biomimetic peptides such as HAV and RGD peptides on the chondrogenic differentiation of hMSCs cannot be separated from those of the chondrogenic environment (chondrogenic medium) [28,29]. To ensure that hMSCs in hydrogels exhibit similar chondrogenic differentiation to that seen in the natural ECM, and are thus suitable for *in vivo* applications, mature and reliable

inducers need to be included. Kartogenin (KGN), a small-molecule organic compound, exhibits great potential for promoting chondrocyte proliferation and chondrogenesis of hMSCs [30,31]. Compared to protein growth factors, KGN shows physicochemical stability in different environments [32]. However, due to the low water solubility and hydrophobic nature of KGN, it cannot be efficiently loaded in highly hydrophilic hydrogel systems [33]. Furthermore, a growing number of reports have shown the importance of the timing of biological signals for cell differentiation [34,35]. Therefore, it is necessary to package KGN with other carriers to achieve effective and continuous release manner, which is required for microenvironment of cartilage regeneration [36,37].

In this study, stem cells were first regulated by RGD peptides, to enhance interactions with the matrix; then, a gel with an appropriate swelling ratio and elastic stress was used to promote cell proliferation and aggregation in the gel. We hypothesized that cells migrate and aggregate in the stromal environment through intercellular interactions mediated by HAV peptides. Whether these peptides mediating cell proliferation and aggregation can better regulate chondrogenic differentiation of hMSCs and promote matrix deposition remains to be demonstrated. On the basis of the above research, introducing biological cues prompting the chondrogenic differentiation of hMSCs at the appropriate time is imperative, to better simulate microenvironment of chondrogenesis. By controlling the release of KGN encapsulated in microspheres, we can determine its effect on hMSCs chondrogenesis. This could have value in cartilage tissue engineering applications.

2. Experimental section

2.1. Preparation of functionalized hyaluronic acid hydrogels

HA (66–90 kDa; Lifecore, Chaska, MN, USA) was modified with methacrylate, as described previously [28]. Briefly, the hydroxyl of the HA was reacted with methacrylate anhydride in 10-fold excess. Then, 1 g of HA was dissolved in 100 ml of deionized water and dripped with methacrylic anhydride (Sigma-Aldrich, St. Louis, MO, USA). The reaction pH was adjusted to between 8 and 9 with 5 M sodium hydroxide, and the reaction proceeded for 24 h in an ice bath. The resulting MeHA was dialyzed for 3 days, freeze-dried, and stored at −20 °C. The degree of MeHA methacrylation was determined by proton nuclear magnetic resonance (^{1}H NMR) spectroscopy. MeHA solution (1%, w/v) was obtained by dissolving MeHA into Irgacure 2959 aqueous solution (0.1%, w/v). Then, above mixed solution was irradiated for different time using a UV light (365 nm, 1 W) to form hydrogel.

2.2. Peptide coupling to MEHA

RGD peptide (sequence GCGYRGDSPG) and HAV peptide (sequence Ac-HAVDIGGC) were purchased from China Peptides Co. Ltd. (Shanghai, China) and synthesized by a batch-wise 9-fluorenylmethyloxycarbonyl (FMOC)-polyamide method with a purity of at least 98%. Briefly, MeHA and peptides were dissolved in a 0.2 M triethanolamine (TEOA) buffer (pH 8.0) for an overnight reaction at 37 °C, followed by dialysis for 3 days, freezing, and lyophilization. The amount of RGD or HAV peptide used was set to 112 μmol/g HA. The coupling peptide reaction did not consume more than 20% of the available methacrylate groups.

2.3. Characterization of functionalized hyaluronic acid hydrogels

For elastic modulus measurement, hydrogels with different degrees of crosslinking were immediately subjected to an unconfined compression test (1 mm/min) in a mechanical apparatus (Electro-Force 3100; BOSE, Framingham, MA, USA) at room temperature.

For swelling ratio measurement, hydrogels with different degrees of crosslinking were immersed in phosphate-buffered saline (PBS), fully swollen in a shaking incubator at 37 °C for 24 h, and then weighed to determine the swelling ratio.

After liquid nitrogen freezing and freeze-drying, the 3D porous structure of the hydrogels with different degrees of crosslinking were observed using scanning electron microscopy (SEM) (S-4800, Hitachi, Tokyo, Japan).

2.4. Fabrication of KGN-encapsulated PLGA microspheres (KGN@PM)

The single oil-in-water (O/W) emulsion/solvent evaporation method was used to prepare PLGA microspheres (PMs) [38]. First, 45 mg PLGA (actide/glycolide (50:50); MW, 40−75 kDa) was dissolved in 4.5 ml dichloromethane solution at room temperature for 3 h and 5 mg KGN (Selleck, USA) was dissolved in 0.5 mL of acetone. The two solutions were then mixed together and the resulting solution was slowly dripped into 0.1%, 50 ml chitosan solution stirred by a manual high-speed homogenizer (TH; Omni, Omni International, Marietta, GA, USA), 30,000 rpm, in an ice bath. Finally, the emulsion was dropped into 0.1% 150 ml chitosan solution at 400 rpm overnight. PMs were collected using an ultrafast centrifuge (12,000 rpm, 30 min). After centrifugation, the microspheres were washed three times with deionized water and then freeze-dried and preserved.

2.5. Analysis of KGN release and the encapsulation rate of PM

KGN encapsulated in HR hydrogel, PM, and PM-HR hydrogel were placed in PBS solution, and then in a 37 °C shaking incubator at 100 rpm. The solution was collected by centrifugation and the KGN content was measured by high-performance liquid chromatography (HPLC; [1260 Infinity]; Agilent, Santa Clara, CA, USA). The injection volume was set at 10 μl. The samples were analyzed using a reverse phase column (4.6 × 100 mm, 3.5 μm) and the mobile phase was prepared with acetonitrile/water (v/v, 40/60) plus 0.1% formic acid. The CPT absorbance was monitored at 275 nm and the flow rate was set to 1 ml/min (37 °C). To determine the encapsulation rate of KGN in PM, the supernatant and washing solution were collected and analyzed.

2.6. Evaluation of cell activity *in vitro*

2.6.1. Cell culture

HMSCs were derived from human bone marrow and purchased from ScienCell Research Laboratories (Catalog Number: 7500, Carlsbad, CA, USA). HMSCs were cultured with high-glucose Dulbecco's modified Eagle's medium (DMEM; HyClone, USA) containing 10% fetal bovine serum (FBS, Gibco; Thermo Fisher Scientific, USA) and 1% (v/v) penicillin/streptomycin (Gibco), and were expanded to passage 4–5 for use.

2.6.2. Gel-based 2D and 3D cell culture

For two-dimensional (2D) cell culture, hydrogels were firstly formed at the bottom of 24-well plates. The digested cells were placed on the surfaces of various hydrogels at a density of 2 × 10⁴ cells per well. Then, 1.5 ml medium was added to each well for cell culture, and the liquid was changed once a day.

For hydrogel-based 3D culture studies, the digested cells were centrifuged, and then the supernatant was removed. The cells were resuspended with a gel solution (eventually reaching a concentration of 1 × 10⁶ cells/500 μl). The cell-gels solution (400 μl/well) formed hydrogel at the bottom of ultra- low attachment 24-well

plates. Then, 1.5 ml medium was added to each well, and the liquid was changed once a day.

2.6.3. Proliferation and live/dead assay of hMSCs in gel-based 2D and 3D culture

The proliferation of hMSCs in gel-based 2D and 3D culture was evaluated by the cell counting kit-8 assay (CCK-8, Dojindo, Japan). Briefly, at 1, 3 and 7day *in vitro* culture, CCK-8 reagent was added to the 24-well plate. The incubation solution was incubated in a 5% CO_2 humidified incubator at 37 °C for 3 h and then transferred to a new 96-well plate. Microplate reader (SpectraMax M5) was used to measure optical density (OD) at 450 nm.

For live/dead assay, samples were washed with PBS three times and then added mixed live/dead staining liquid (Dojindo, Japan) for 15 min in a 5% CO_2 humidified incubator at 37 °C. The stained samples were visualized immediately by confocal laser scanning microscopy (CLSM; A1R-si, Nikon, Japan).

2.6.4. Cytoskeletal morphology

The cytoskeletal morphology in the 2D and 3D cell cultures was observed by CLSM. Briefly, after the samples had been fixed with 4% (w/v) paraformaldehyde (Hyclone, Logan, UT, USA) for 30 min, they were washed three times with PBS and then permeabilized with 0.1% (v/v) Triton X-100 (Sigma-Aldrich) for 15 min. After that, the samples were washed three times with PBS and then incubated them with 5 mg/mL fluorescein isothiocyanate (FITC)-phalloidin solution (Sigma-Aldrich) for 30 min, followed by 10 mg/ML 4′,6-diamidine-2-phenylindole (DAPI) solution (Sigma-Aldrich) for 10 min. The stained samples were visualized immediately by CLSM.

2.7. Evaluation of chondrogenic differentiation of hMSCs *in vitro*

To study the chondrogenic differentiation of hMSCs in gel-based 3D culture, the samples were cultured in chondrogenic medium (CM), which consisted of low-glucose DMEM supplemented with 1% penicillin/streptomycin, 100 μg/mL sodium pyruvate, 40 μg/mL L-proline, 50 μg/mL L-ascorbic acid-2-phosphate, 1% insulin-transferrin-selenium (ITS) (Cyagen, Santa Clara, CA, USA), 100 nM dexamethasone, and 10 ng/ml TGF-β3. The CM in all groups was changed every other day.

2.8. Evaluation of chondrogenic differentiation of hMSCs *in vivo*

2.8.1. Subcutaneous implantation of hMSC-laden hydrogels in nude mice

HMSC-laden hydrogels were subcutaneously implanted into male nude mice (aged 6–8 weeks) to investigate the effect of chondrogenic differentiation *in vivo*. HMSCs-laden hydrogels (10 million cells/ml) were directly inserted into subcutaneous pockets on the left and right sides of the back of each nude mouse. Samples were harvested after 4 and 8 weeks. All of the animal procedures used in this experiment were approved by the Animal Care and Use Committee of Peking University.

2.8.2. Histological analysis

After nude mice were euthanized on the 28th and 56th day post-surgery, samples were excised and then fixed with formalin solution overnight. The specimens were dehydrated with gradient ethanol and then embedded in paraffin and cut into 7-μm-thick sections. The sections were process for deparaffinization and rehydration, and then stained with hematoxylin and eosin (H&E) staining, safranin O staining and immunohistochemistry (IHC) staining following the manufacturer's protocol. The primary antibodies for IHC, including Collagen I (GB11022) [Coll I, 1:1000, Servicebio, China]and Collagen X (GB111003) [Coll X, 1:1000, Servicebio]. The

stained samples were viewed under an inverted light microscope (Olympus, Tokyo, Japan).

2.9. Collagen and GAG content and RNA analysis

To determine the GAG content of the hydrogels, the cell-gels were first freeze-dried and weighed (the samples from nude mice were directly weighed and ground without freeze drying). Then, samples were ground manually with a glass grinding tube in 1 ml papain lysate. Then, the above products were incubated at 60 °C for 24 h for subsequent testing. The GAG content was evaluated using dimethylmethylene blue dyes (Sigma-Aldrich).

To determine the collagen content of the hydrogels, the tissues or cell-gels were ground with 6 mol/L HCl hydrolysate, digested in a boiling water bath for 3–6 h and then centrifuged at 15,000 rpm. The supernatant was collected and the pH was adjusted to 6–8. The collagen was quantified using a hydroxyproline (HYP) assay kit (Solarbio, Beijing, China), although HYP only accounts for 13.4% of the total collagen content.

To analyze the RNA in the cell-hydrogel structures, the cell-gels were washed three times with PBS and then ground manually with a glass grinding tube in 1 ml TRIzol (Invitrogen, Carlsbad, CA, USA). After that, the cell-gels were reverse-transcribed into cDNA using the Revert Aid First Strand cDNA Synthesis Kit (Thermo, Waltham, MA, USA). Real-time polymerase chain reaction (RT-PCR) was performed using SYBR green (Roche, Indianapolis, IN, USA) and the ABI 7500 RT-PCR instrument (Applied Biosystems, Foster City, CA, USA). The RNA sequences in this paper are listed in Table S1. 28 sr was used as a housekeeping gene for PCR amplification. The comparative CT ($2^{-\triangle\triangle CT}$) method was applied to evaluate the relative RNA expression.

2.10. Immunofluorescence

After 14 or 28 days of culture *in vitro*, the cell-gels were fixed with paraformaldehyde (4%, w/v) for 30 min and then washed with PBS three times. Hydrogel were permeabilized with Triton X-100 (0.1%, v/v) for 15 min at room temperature (For analysis of the samples *in vivo*, paraffin sections should be deparaffinized, rehydrated and antigen retrieval before immunofluorescence staining). After washing three times with PBS, cells were incubated with 3% (w/v) bovine serum albumin solution (Sigma-Aldrich) for 2 h at room temperature. Afterwards, cells were incubated with primary antibodies (Rabbit Anti-Integrin $\beta1$ antibody (ab183666) [1:200, Abcam, UK], Mouse Anti-N Cadherin antibody (ab98952) [1:200, Abcam], Rabbit Anti-NCAM1 antibody (ab133345) [1:100, Abcam], Mouse Anti-Aggrecan antibody (ab3778) [ACAN, 1:50, Abcam], Rabbit Anti-Collagen II antibody (ab34712) [Col II, 1:200, Abcam], at 4 °C overnight. After three washes with PBS, sample were incubated with secondary antibodies at a dilution of 1:500 for 2 h in the dark at room temperature [goat anti-rabbit IgG H&L (Alexa Fluor 488), goat anti-rabbit IgG H&L (Alexa Fluor 568), goat anti-mouse IgG H&L (Alexa Fluor 647), Abcam]. Finally, cell nuclei were stained with DAPI for 10 min at room temperature. The stained samples were visualized immediately by CLSM. Quantitative analysis of immunofluorescence staining was analyzed using ImageJ software (NIH, Bethesda, USA) [39].

2.11. Statistical analysis

Data is presented as the mean ± standard deviation and represents three individual experiments. Statistical analysis was conducted by one-way analysis of variance (ANOVA) followed by Tukey's post hoc tests using SPSS 24.0. P-value less than 0.05 was considered statistically significant.

3. Results and discussion

3.1. Preparation and characterization of functionalized hydrogel

Studies have increasingly focused on how cells behave in tissue-engineered scaffolds. In particular, as a biomimetic 3D culture system, functional hydrogels have become popular in the regulation of cell signaling and behavior [40]. The activities of MSCs can be adjusted by modifying active groups [41], introducing active signals into the hydrogel system [42], and changing the structure of the gel [43]. In the field of cartilage tissue engineering, the complicated process of differentiating MSCs into chondrocytes must be comprehensively investigated to guide the preparation of hydrogel scaffolds. However, few studies have used hydrogel scaffolds to mimic the critical steps in chondrogenic differentiation, namely spontaneous cell proliferation, condensation, and differentiation, and matrix precipitation. It is also worth noting that these critical stages are not independent elements of the chondrogenic differentiation process. Cell condensation usually occurs after a large number of cells have been amplified, and is indispensable for cell differentiation [24,25] (Fig. 1A). Therefore, it is imperative to incorporate these key links into functional design of hydrogels.

At the beginning of this study, HA reacts with excess methacrylate to produce double bonds to ensure the quality of grafted peptides and stability of the glue (Fig. 1B). Through NMR analysis, we confirmed that the "double bond binding rate" of HA was about 43% (Fig. S1). Swelling and elastic stress tests showed that grafting peptides onto MeHA did not affect swelling or elastic strain (Fig. 1C and D), consistent with previous reports [28]. The effect of crosslinking time on the characteristics of gels showed that the elastic modulus of the gel matrix increased with longer crosslinking time (Fig. 1C). The group with crosslinking of 30 s had the lowest mechanical stress, highest swelling ratio, and notable volume changes after swelling (Fig. 1C and D, Fig. S4 A). When the crosslinking time was 60, 90 or 120 s, the swelling ratio was lower, and the volume relatively stable, compared to the 30 s group. Appropriate volume changes may be important for the repair and regeneration of cartilage defects (Fig. S4). A high swelling ratio cause a distinct change in gel volume after the formation of hydrogels in cartilage defect. On the contrary, high crosslinking strength with a low swelling ratio maintained the gel volume before and after swelling, which may help to close the cartilage defect. Therefore, we hypothesized that crosslinking of 60 s or more would contribute to the stability of gel volume and clinical application.

The SEM images showed that the pores of lyophilized gels with more than crosslinking of 60 s were smaller than those in the 30 s and 60 s group (Fig. 1E). The pores in the lyophilized hydrogels prepared in this study were all on the order of microns. However, the freeze-dried hydrogels can hardly reflect the actual structure and size of pores in the hydrated state [44,45]. It is worth noting that the lower degree of crosslinking leads to larger pore size of hydrogels, and the hydrogels with larger gaps tend to be closely associated with promoting cell differentiation, proliferation, and aggregation, as well as matrix secretion [46,47].

3.2. Spreading and proliferation of hMSCs loaded on hydrogel surfaces and encapsulated in hydrogels

By studying the elastic moduli and swelling ratio of gels with different degrees of crosslinking, we showed that hydrogels with suitable crosslinking strengths (60 s, 90 s and 120 s) may merit further research. Then, we investigated the effect of crosslinking intensity on cell survival. HMSCs encapsulated into MeHA hydrogel with different degrees of crosslinking were cultured *in vitro* for 7 days, and dead cells were not revealed by dead-live staining (Fig. S2).
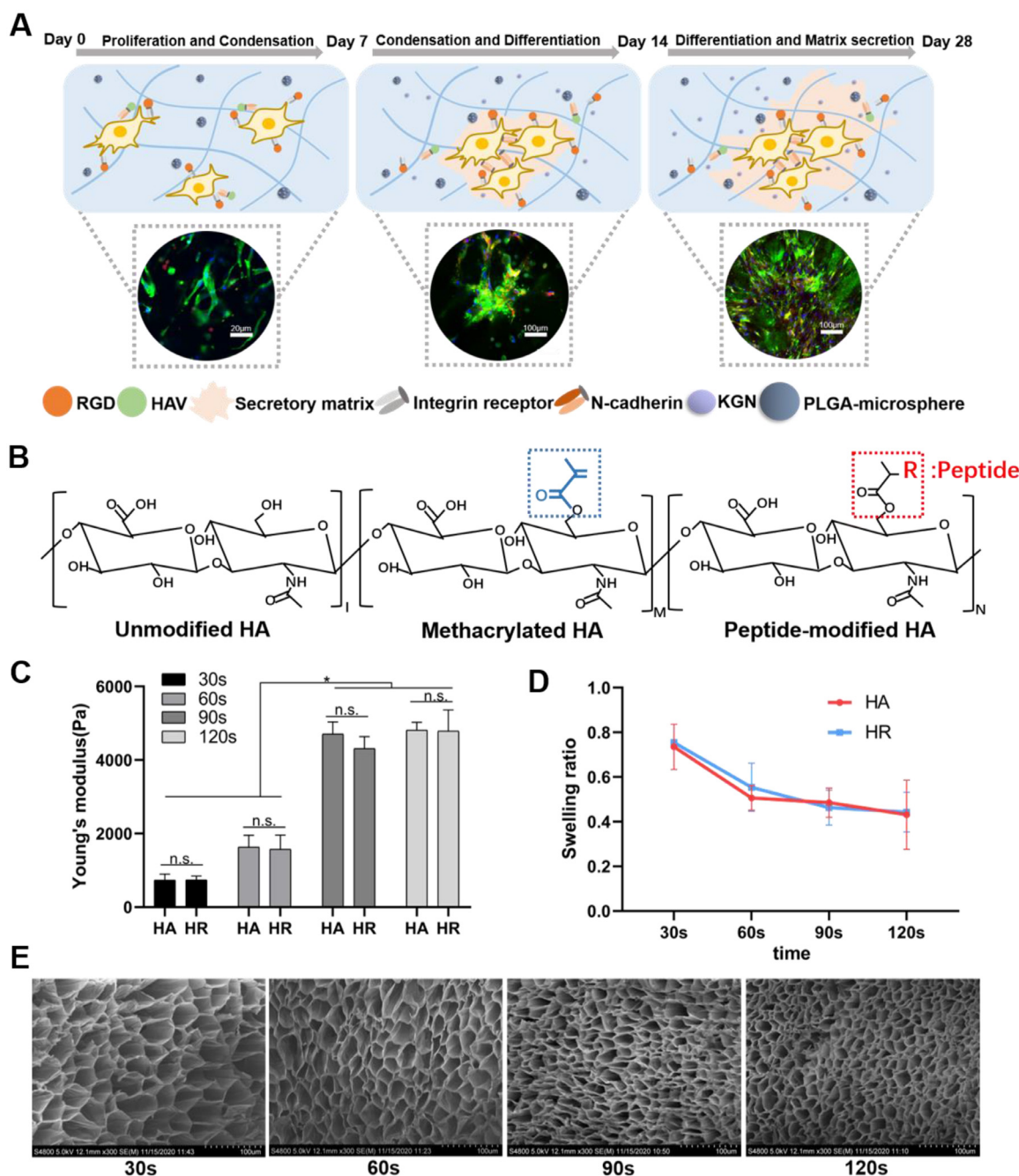
Fig. 1. Preparation and characterization of functionalized hydrogel. (A) Schematic illustration of the K@PM-HR hydrogel for inducing hMSC chondrogenesis. (B) HA modified with methacrylates, and MeHA grafted with peptides. (C) Elastic modulus of grafted and ungrafted peptide hydrogels. (D) The swelling ratio of grafted and ungrafted peptide hydrogels. (E) Representative SEM images for different crosslinking times. Scale bar=100 μm. Data are shown as mean $\pm$ SD.; n = 3. * < 0.05, n.s. P>0.05.

Natural ECM regulates cell phenotype, activity, and proliferation through ECM ligands [20,48]. This can be replicated by incorporating RGD peptides into hydrogels. In this study, we demonstrated that a 2% concentration of gel modified with RGD inhibited cell spreading compared to a 1% concentration (Fig. S3). Further studies were carried out to investigate whether RGD peptides have different effects on cells in gels varying in the degree of crosslinking. At the 2D level, compared to the HA group, the RHA group enhanced cell adhesion, spreading, and proliferation after 3 days of cell culture on the surface of the hydrogel. The cells produced similar cellular states on the surfaces of hydrogels with different crosslinking strengths in HA or RHA group (Figs. 2A and B, 3A and B). In the case of 3D samples, the cells in all HA groups were isolated in the gel matrix and showed a spherical shape with no intercellular contact, regardless of the crosslinking strength (Fig. 2C and E). Meanwhile, although there is a tendency of cell proliferation with the growth of culture time, different crosslinking intensity did not have different effects on cell proliferation in the HA group (Fig. 3C). In particular, the proliferation amplitude of cells in all HA groups was less pronounced than in the RHA group (Fig. 3C and D). On the other side, the cells in the RHA group exhibited different morphologies and activities according to the degree of crosslinking (Fig. 2D and F, Fig. 3D). In the groups with crosslinking of 30 s and 60 s, the cells extended well and exhibited higher proliferative ac-
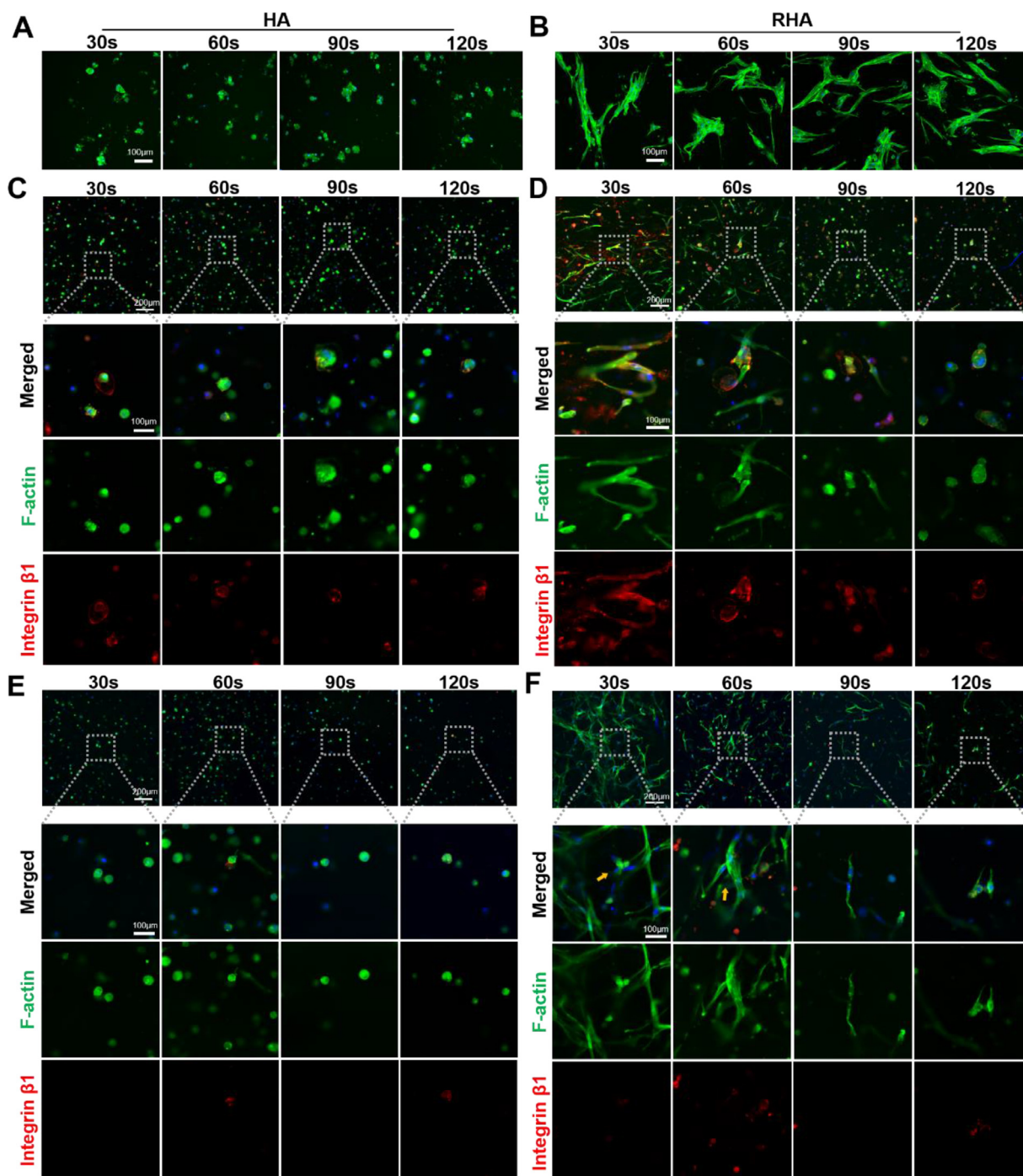
Fig. 2. Representative images of hMSCs encapsulated in 2D substrates and 3D matrices. (A) Morphology (F-actin) of hMSCs on the surface of HA according to different crosslinking times after 3 days of culture. (B) Morphology of hMSCs on the surface of RHA according to different crosslinking times after 3 days of culture. (C) Morphology and integrin β1 expression of hMSCs in 3D HA matrices with different crosslinking times after 3-days of culture. (D) Morphology and integrin β1 expression of hMSCs in 3D RHA matrices with different crosslinking times after 3 days of culture. (E) Morphology and integrin β1 expression of hMSCs in 3D HA matrices according to different crosslinking times after 7 days of culture. (F) Morphology and integrin β1 expression of hMSCs in 3D RHA matrices according to different crosslinking times after 7 days of culture (yellow arrows: cell aggregation). (For interpretation of the references to colour in this figure legend, the reader is referred to the web version of this article.)

tivity (Fig. 2D and F, Fig. 3D). Meanwhile, the cells began to spread and migrate on the third day of culture (Fig. 2D), and distinct aggregation was noted on day 7 (Fig. 2F). Longer crosslinking times (90 and 120 s) limited cell spreading, migration and proliferation (Fig. 2D and F, Fig. 3D), leading to a nearly spherical cell morphology (Fig. 2D), similar to the cells in the HA group.

After 3 days of cell culture, compared to the HA group, the expression of integrin receptors was upregulated in the RHA group.

Moreover, with the participation of RGD peptide, the expression of integrin receptors was more obvious in low cross-linked matrixes than in high cross-linked matrixes (Figs. 2C-F 3E and F). Material-bound RGD peptides can increase adhesion of the matrix to cells, which mimics the relationship between the natural matrix and cells. Importantly, high expression of integrin indicates the initiation of cell proliferation and differentiation [49]. When cells are encapsulated inside the material, they tend to prolifer-
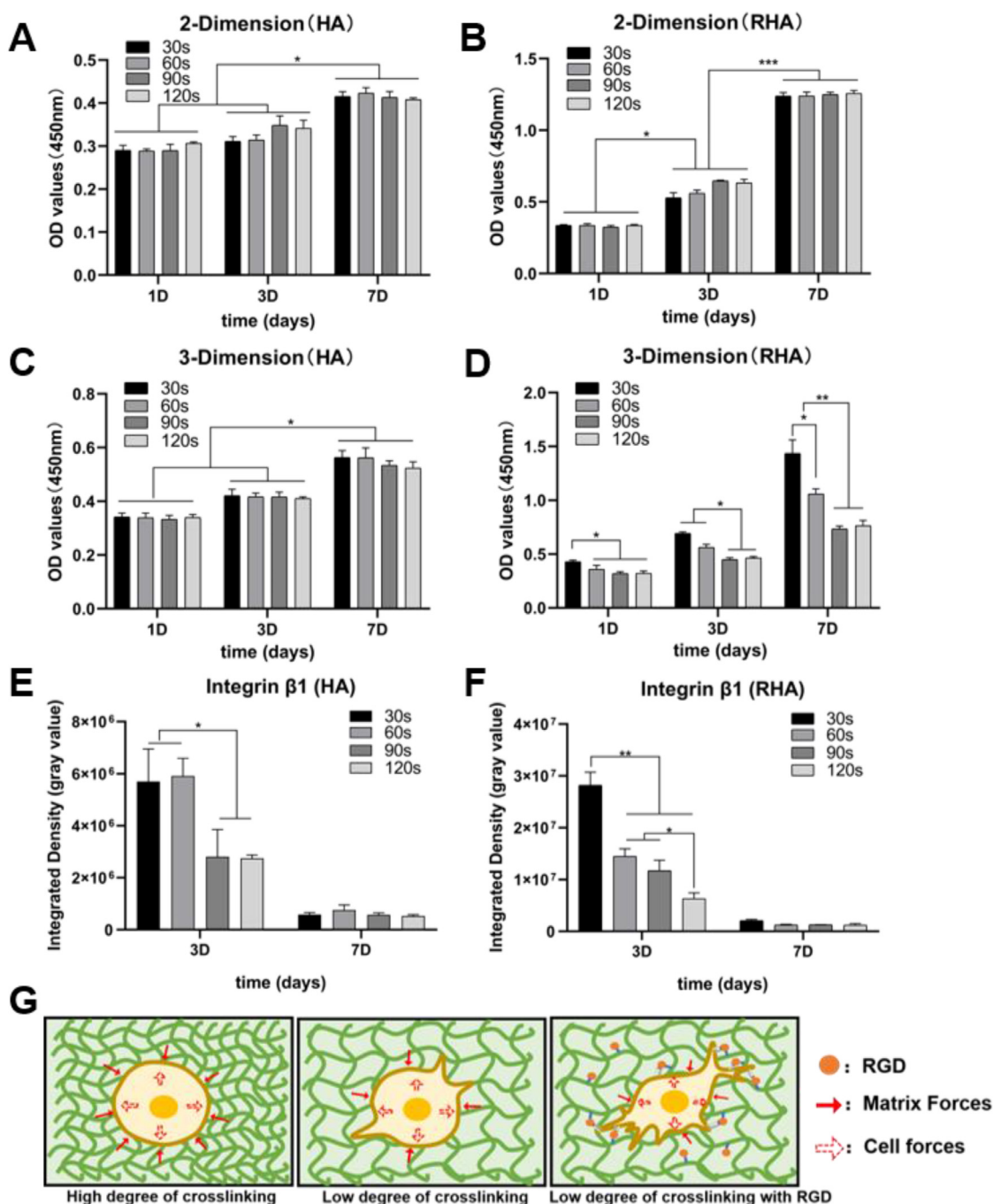
Fig. 3. Proliferation and activity of hMSCs encapsulated in 2D substrates and 3D matrices. (A, B) Proliferation of hMSCs on HA and RHA surfaces according to different crosslinking times. (C, D) Proliferation of hMSCs in 3D HA and RHA matrix surfaces according to different crosslinking times. (E, F) The analysis of integrin $\beta 1$ expression in HA or RHA group by fluorescent intensity (G) Schematic diagrams of cell-matrix interactions according to the degree of crosslinking. Data are shown as mean $\pm$ SD; $n = 3$. * < 0.05, ** < 0.01, *** < 0.001.

ate, migrate, and aggregate. ECM ligands direct these cell behaviors, but a high degree of crosslinking produces a robust matrix that binds to the cells inside it, thereby inhibiting such behaviors (Fig. 3G). The dynamic interaction between the cells and gel matrix is favorable for cell differentiation [50,51]. In this experiment, the RHA groups with low crosslinking strength produced a soft matrix; thus, the gel matrix induced a remodeling process via cell movement. Notably, the expression of integrin receptors decreased significantly after 7 days of culture in all groups (Fig. 2E and F). This may have been due to the consumption of RGD peptides by inte-

grin receptors, accompanied by the degradation of RGD and integrin [52,53].In addition, it is undeniable that the stiffness of hydrogel in this study is very soft, while the implants for cartilage defect often depend on scaffolds with high elastic modulus [54]. There is a conflict between the regulation of MSC activity by functional gel matrix and the high elastic modulus of gel matrix [22,40]. On the basis of regulating the cell activity, it is an effective solution to increase the mechanical stress through matrix secretion [28,36], but there is still a significant gap with the stiffness of natural cartilage tissue.
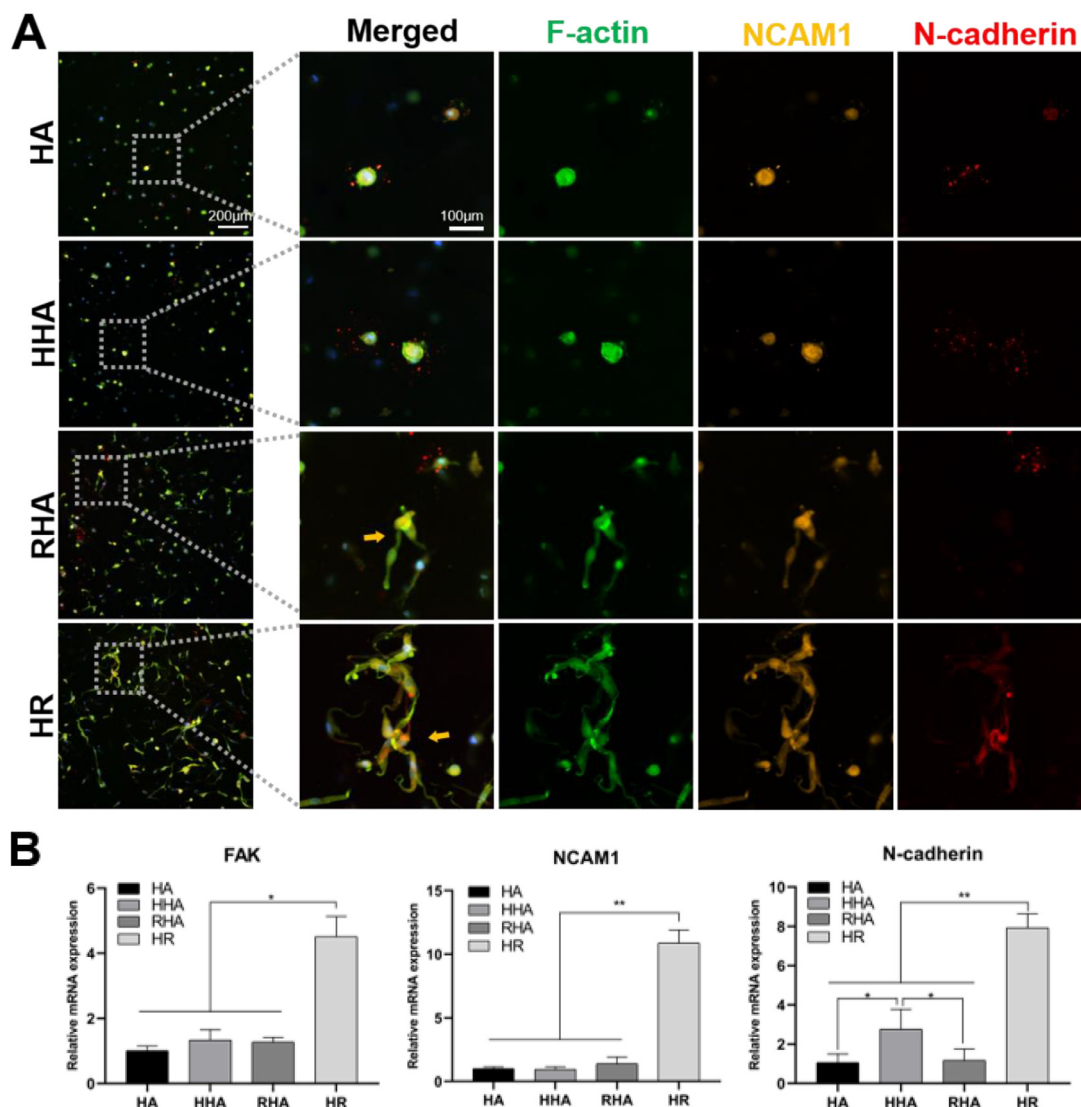
Fig. 4. The analysis of mesenchymal condensation after 3 days of culture. (A) Immunofluorescence staining for cytoskeleton (F-actin), NCAM1, and N-cadherin (yellow arrows: cell aggregation). (B) Expression of FAK, NCAM1 and N-cadherin after 3 days of culture. Data are shown as mean ± SD; $n = 3$. * < 0.05, ** < 0.01. (For interpretation of the references to colour in this figure legend, the reader is referred to the web version of this article.)

3.3. Grafting peptides affect cell condensation

To verify the regulatory effect of grafted HAV on stem cell aggregation and investigate the effect of two types of peptides (RGD and HAV) on cell behaviors, the expression levels of proteins and genes related to cartilage adhesion (NCAM1 and N-cadherin) and migration (FAK) were evaluated. After 3 days of culture, immunofluorescence staining clearly showed that, little cell aggregation was observed in the early stages in the HAV group (Fig. 4A) and the expression of NCAM1 and N-cadherin were highest in the HR group (Fig. 4A, Fig. S5). In the RHA and HR groups, cells aggregated locally in small areas (Fig. 4A). Previous studies have shown that gel matrix of pure MeHA does not promote the aggregation of MSCs under the influence of HAV peptide, especially in early culture [27,28]. This also indicates that a suitable hydrogel matrix microenvironment is required to exert the effect of HAV on MSCs. In terms of gene expression, grafted RGD peptides alone did not promote significant early expression of FAK and NCAM1, while grafted HAV peptides promoted greater upregulation of N-cadherin

compared to the blank control and RHA groups (Fig. 4B). High expression of N-cadherin is associated with active MSC aggregation, which is believed to be a prerequisite for neocartilage formation [55,56]. It should be noted that, compared to other groups, the expression of FAK, NCAM1, and N-cadherin were greater in the HR groups (Fig. 4B). The upregulation of these adhesion-related genes also indicates chondrogenic differentiation [15,24]. Simultaneous grafting with both types of peptide had a synergistic effect on cell adhesion and migration, although the underlying mechanism is unclear. It is most likely that RGD peptides promote cell proliferation and migration, where cellular motion-mediated cell-cell interactions upregulate proteins and genes related to intercellular adhesion [57–59].

3.4. KGN release

Regarding the release behavior in different media (Fig. 5B), about 80% of the total amount in the HR group was released within the first 7 days. This indicates that functional hydrogel matrix
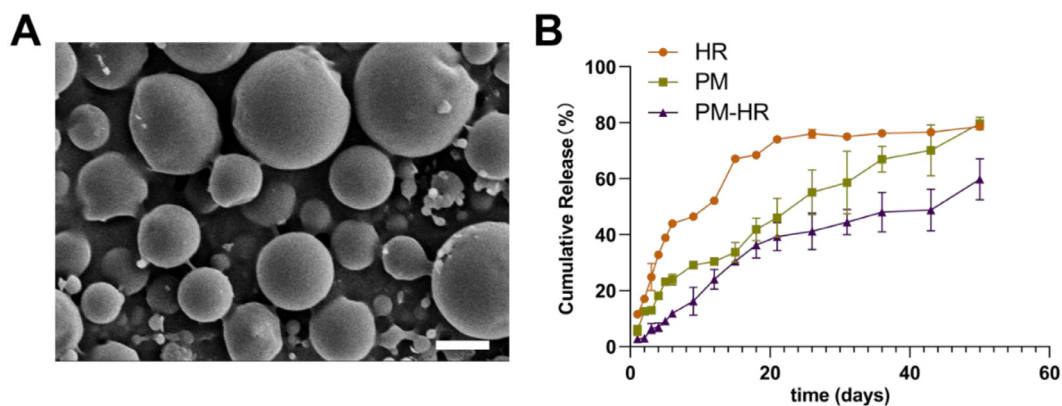
Fig. 5. Characterization of KGN encapsulated in peptide-modified hydrogel (HR), PMs (PM) and PMs integrated with hydrogel(PM-HR). (A) SEM image of the KGN-encapsulated PMs. Scale bar = 2 μm (B) Release kinetics of KGN encapsulated in peptide-modified hydrogel, PMs and PMs integrated with hydrogel.

could not store hydrophobic KGN effectively. The release of KGN wrapped in PMs was delayed compared to the HR group (Fig. 5A and B). As expected, K@PM wrapped in gel had the lowest release rate, which ensured a constant concentration of KGN in the gel system.

3.5. Chondrogenesis and secretion of hMSCs encapsulated in hydrogel in vitro

Immunofluorescence staining showed that the number of nuclei indirectly reflected the number of cells after *in vitro* culture for 14 days (Fig. 6A, DAPI staining). In the RHA, HR, K@HR and K@PM-HR groups, the number of cells increased significantly over time and more obvious aggregation was observed, at 14 *versus* 7 days (Fig. 2F). At the same time, cartilage-related proteins were clearly expressed in all groups with RGD and HAV peptides (Fig. 6A, F and G). Notably, cartilage-related collagen II (Coll II) and aggrecan (ACAN) were clearly expressed in the group with KGN, suggesting that KGN promoted chondrogenic differentiation of hMSCs (Fig. 6A, F and G). In terms of gene expression, the gels grafted with RGD and HAV peptides significantly upregulated the expression of ACAN, Coll II and sex-determining region Y-box 9 (SOX-9) compared to the HA, HHA and RHA groups (Fig. 6B–E). Prior upregulation of genes related to cell migration and aggregation in the HR group at 3 days was fed back into chondrogenic differentiation. There was no evident group difference in ACAN or Coll II expression, but the expression of SOX-9 and collagen X (Coll X) was markedly upregulated in the RHA group compared to the HHA group (Fig. 6B–E). Particularly, high expression of Coll X indicating hypertrophy is not conducive to chondrogenesis and cartilage repair [60]. The upregulation of hypertrophy genes in the HR, K@HR and K@PM-HR groups may be related to the RGD peptides in hydrogel matrix. Previous studies have also shown that RGD incorporated into hydrogel matrix can up-regulate hypertrophy-related genes of MSCs [29,46]. In the K@HR and K@PM-HR groups, the expression levels of ACAN, Coll II, and SOX-9 were upregulated. Meanwhile, the expression level of SOX-9 was highest in the K@PM-HR group. The above results, obtained after 14 days of culture, appear to confirm that our hydrogel system can continuously promote the proliferation, aggregation and development of hMSCs into chondrocytes.

Immunofluorescence staining showed that the number of cells after 28 days of *in vitro* culture was visibly increased compared to that at 14 days, especially in the RHA, HR, K@HR and K@PM-HR

groups. Moreover, cell aggregation was more obvious and more extensive than at 14 days (Fig. 6J). The expression of Coll II and ACAN was significant in all groups (Fig. 6J, O and P). Subsequently, the expression of cartilage-related proteins, accompanied by wide intercellular contact, was obviously higher in the K@HR and K@PM-HR groups than in HA, HHA and RHA groups (Fig. 6J, O and P). The degree of hMSC chondrogenesis depends on the extent of intercellular contact, and is linearly correlated with the number of adjacent cells [15,25]. At this point, the expression of type II collagen was the highest in K@PM-HR group (Fig. 6P). Regarding gene expression, gels grafted with RGD and HAV peptides significantly upregulated the expression of ACAN and Coll II compared to the HA, HHA and RHA groups (Fig. 6K–N). The expression of ACAN and Coll II was upregulated in the RHA and HHA groups compared to the HA group, but there was no difference in the expression of SOX9 between the RHA and HHA groups. By comparing the K@HR and K@PM-HR groups, it was clear that sustained release of KGN had the most profound effect on the upregulation of cartilage-related genes, suggesting that this way of releasing is favorable to the formation of neo-cartilage (Fig. 6K-N). The clear upregulation of chondroblast-related proteins and genes in the K@HR and K@PM-HR groups reflected enhancement of chondrogenesis via the synergistic effects of KGN and ECM, consistent with the results reported in previous studies [61–63]. Notably, hypertrophy genes were still highly expressed in the HR, K@HR and K@PM-HR groups (Fig. 6M). At the same time, with the high expression of hypertrophy gene, collagen I (Coll I) associated with osteogenesis was significantly expressed in K@PM-HR group after chondrogenic induction of 14 and 28 days *in vitro* (Fig. 6D and M, Fig. S6). Up-regulation of Coll I and Coll X predicts endochondral ossification [64]. Normally, MSCs gradually become chondrocytes after proliferation and condensation. When chondrocytes further mature, some of them from the center of the cartilaginous anlage differentiate into hypertrophic chondrocytes that secrete Coll X and facilitate calcification of matrix. Next, hypertrophic chondrocytes can regulate angiogenesis and synthesize osteogenic factors. Eventually, bone tissue forms within the hypertrophic cartilage [65–67]. In this system of functionalized hydrogel, formation of mature cartilage may involve endochondral ossification pathways. Even so, the expression of hypertrophic and osteoblastic genes was still low compared with the expression of cartilage-related genes in K@PM-HR group (Fig. 6B-E and K-N, Fig. S6). All in all, the result indicates that this functional HA scaffold can play an advantage in endochondral ossification, which needs to be further comprehensively demonstrated.
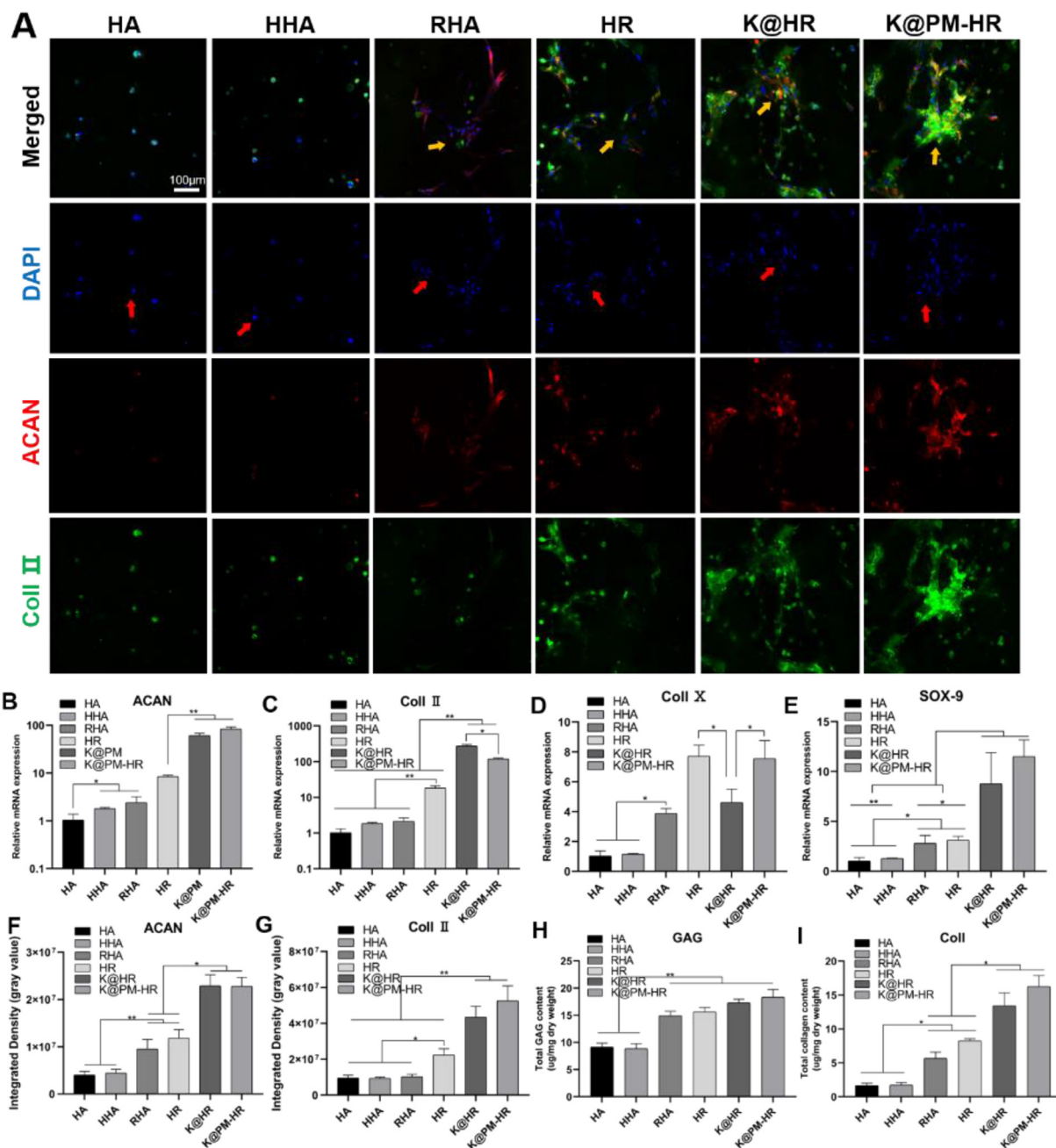
Fig. 6. Evaluation of chondrogenesis after 14 days (A-I) and 28 days (J-R) of chondrogenic culture. (A, J) Immunofluorescence staining for chondrogenic-related proteins in the different groups (yellow arrows: cell aggregation; red arrows: cell nucleus). (B–E, K-N) Gene expression of chondrogenic-related genes in the different groups. (F, G and O, P) The analysis of ACAN and Coll Ⅱ expression in the different groups by fluorescent intensity (H, I and Q, R) Quantitative analysis of collagen and GAG content in the different groups. Data are shown as mean ± SD; $n = 3$. * < 0.05, ** < 0.01, *** < 0.001. (For interpretation of the references to colour in this figure legend, the reader is referred to the web version of this article.)

The main components of the cartilage matrix, such as GAG and collagen, maintain the phenotype of cells within the matrix and provide support for cartilage [36,68]. Compared to 3D porous scaffolds, there has been little researched on the secretion of hMSCs in hydrogel scaffolds, especially for covalently cross-linked hydrogels. In this study, after 14 days of chondrogenic induction culture, the amounts of GAG and total collagen secreted in the RHA, HR, K@HR and K@PM-HR groups were clearly higher than in the HHA and HA groups (Fig. 6H and I). The secretion of collagen was highest in the K@HR and K@PM-HR groups. On the other side, after 28 days of chondrogenic induction (Fig. 6Q and R), the amounts of GAG

and collagen secreted in the RHA, HR, K@HR and K@PM-HR groups were observably higher than in the HHA and HA groups, in which the secretion amounts remained very low. The GAG secretion in the K@PM-HR group was observably higher than in RHA, HR and K@HR groups. Through quantitative analysis and direct observation by light microscopy (Fig. S7 and S8, Fig 6), we determined that our hydrogel system facilitated matrix secretion due to the involvement of RGD peptides and the mechanical properties of hydrogel matrices, and promoted the differentiation of hMSCs. Additionally, with the exception of GAG secretion in HA and HHA group, the matrix secretion increased markedly at 28 days compared to 14
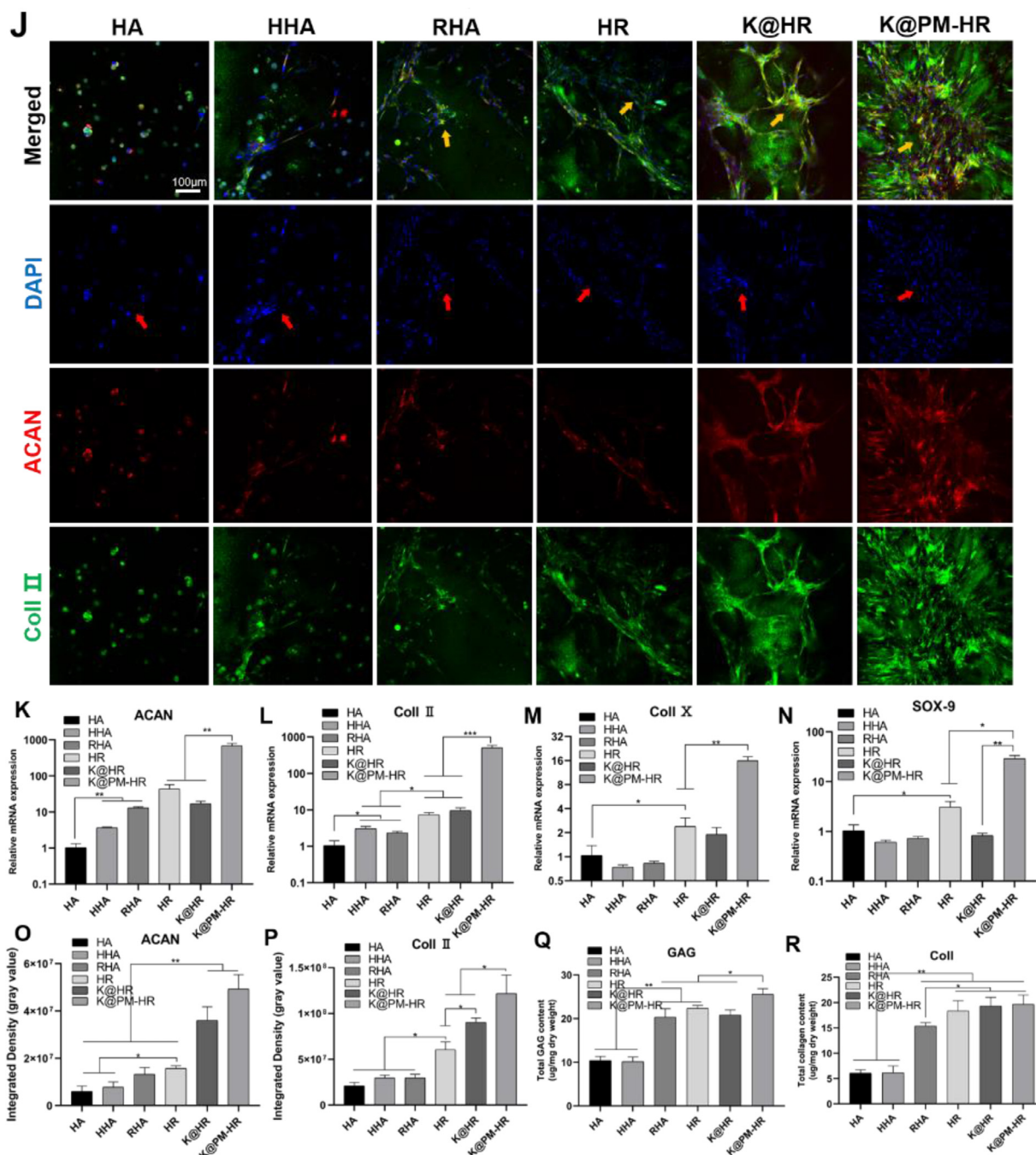
Fig. 6. Continued

days (Fig. S9). Although the quantity of cartilaginous matrix secretion in the HHA group did not significantly differ from that in the HA group (Fig. 6Q and R), light microscopy revealed cell condensation and local matrix secretion with long-term culture (at 28 days) in the HHA group (Fig. S8). These results are similar to those of previous report, that is, HAV peptides grafted onto MeHA hydrogel can regulate hMSCs secretions with long-term culture during the process of neo-cartilage formation [28].

3.6. Chondrogenesis and secretion of hMSCs encapsulated in hydrogel in vivo

To further investigate whether our hydrogel system promoted stem cell activity and chondrogenic differentiation *in vivo*, high-

density cells encapsulated in different gels were implanted subcutaneously in nude mice (Fig. 7A). At 56 days after implantation, the HR, K@HR and K@PM-HR groups secreted a more opaque matrix than the blank control group (Fig. 7A). Compared to the HR group, specimens from the K@HR and K@PM-HR groups were more compact and brighter, similar to cartilage. This result is related to the addition of KGN, which played a role in regulating chondrogenic differentiation and promoting secretion of cartilaginous matrix. H&E staining revealed that the composition of the matrix in the blank control group changed little between 28 and 56 days, and was similar to that of the gel (Fig. 7B). The HR, K@HR and K@PM-HR groups exhibited a wider cell distribution and more stromal secretions (Fig. 7B). Furthermore, H&E staining and immunofluorescence confirmed that the specimens were wrapped in
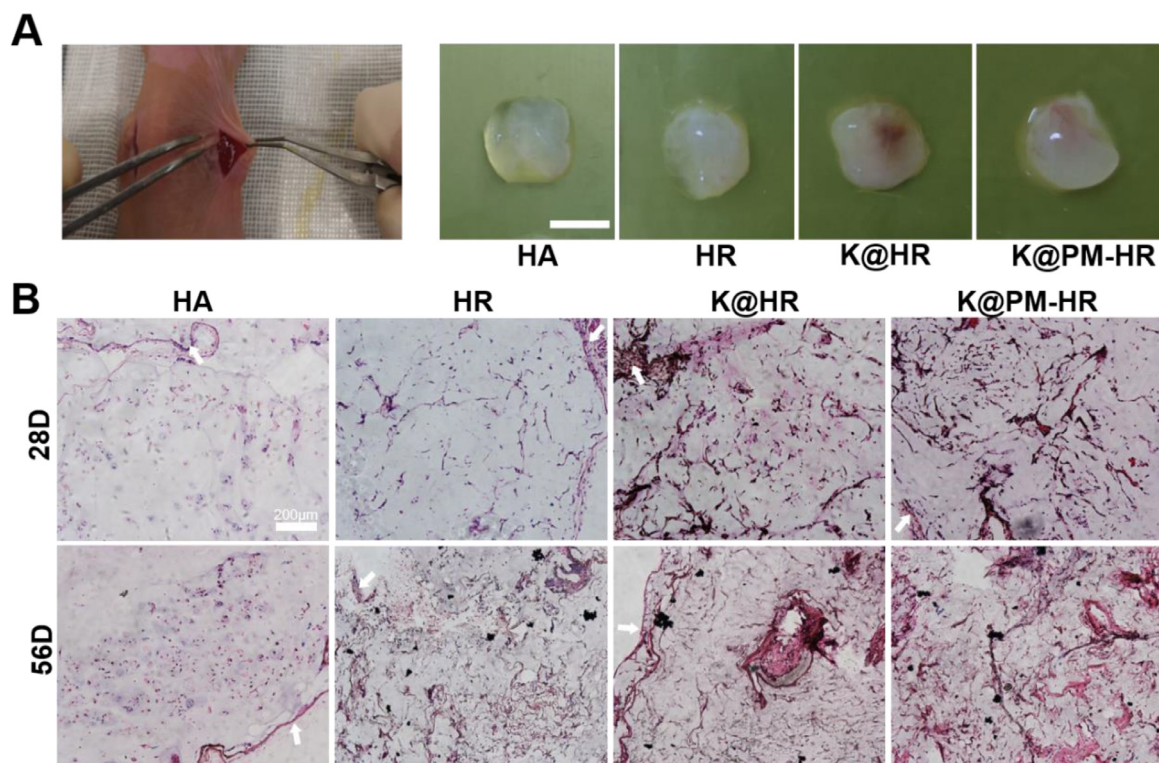
Fig. 7. Harvested hMSC-laden hydrogel implants in nude mice after subcutaneous implantation. (A) Gross view of surgical implantation and hMSC-laden hydrogel implants after 56 days of subcutaneous implantation. Scale bar = 5 mm. (B) H&E staining for hMSC-laden hydrogel implants 28 and 56 days after subcutaneous implantation (white arrows: fibrocystic layers). Scale bar = 200 μm.

fibrocystic layers including blood vessels and cells, due to the un-avoidable foreign body reactions seen in nude mice [69]. It is not difficult to see that, although the hMSCs-laden hydrogels were implanted in subcutaneous culture for 56 days, the main structure of the sample is still similar to the structure of hydrogel (Fig. 7A) [70]. Tissue composition and cell morphology similar to cartilage tissue could not be seen in these specimen slices. The experiment of subcutaneous implantation plays an auxiliary role in verifying the results and subsequent *in situ* defect experiments in animals are still necessary [33,37].

The weights of the blank control groups were lower than that of other groups on the 28th and 56th day. On the 56th day, the weights of the K@HR and K@PM-HR groups were significantly higher than those of the blank control and HR groups (Fig. 8A). The increase in specimen weight was associated with the amount of stromal secretion. At this point, quantitative analysis of the matrix components demonstrated that more GAG and collagen were secreted in the HR group than in the blank group. After 28 and 56 days of subcutaneous culture, secretions of GAG and collagen were higher in the K@HR and K@PM-HR groups than in HR group. Meanwhile, collagen secretion in the K@PM-HR group was highest on day 56 (Fig. 8A). The immunofluorescence staining results were consistent with the quantitative analysis (Fig. 8B and C, Fig. S10). On the other side, DAPI staining showed that, on days 28 and 56 (Fig. 8B and C), there were more cells in the HR, K@HR and K@PM-HR groups than in the blank control group. In addition, the HR, K@HR and K@PM-HR groups showed a notable increase in cell proliferation between days 28 and 56, while the blank control group exhibited no such change. The results showed the importance of grafted peptides for cell survival and growth *in vivo*. The results of safranin O, ACAN and Coll II staining demonstrated that, when KGN was present in K@HR and K@PM-HR groups, the

Table 1
Abbreviations and preparation of hydrogel.

Abbreviation	Description
HA	MeHA hydrogel only
HHA	MeHA grafted HAV peptide
RHA	MeHA grafted RGD peptide
HR	MeHA grafted HAV and RGD peptide
K@HR	HR hydrogel loaded with KGN
K@PM-HR	HR hydrogel with KGN encapsulated in PLGA microspheres

secretion of cartilage matrix is very obvious (Fig. 8 B and C, Fig. S11 A). In particular, by maintaining KGN at constant and effective concentrations, the chondrogenic differentiation of hMSCs was strengthened (Fig. 8B and C, Fig. S10). The feasibility of our hydrogel system was verified by *in vivo* experiments: the gel system promotes the activity and differentiation of hMSCs, and the production of cartilage matrix. To further supplement and verify the effect of functional hydrogels on endochondral ossification in the subcutaneous environment. Through analysis of IHC staining, it was found that Coll I and Coll X mainly existed in the fibrocystic layers (Fig. S11 B and C). The expression of hypertrophic gene was hardly seen in tissue sections (Fig. S11 B) and, the expression of Coll I can be sporadically seen in specimens (Fig. S11 C). This result is partly explained by the fact that the difference between subcutaneous microenvironment *in vivo* and chondrogenic medium *in vitro* was conspicuous. Some hypertrophy-promoting factors in this medium will inevitably impact the differentiation of hMSCs.
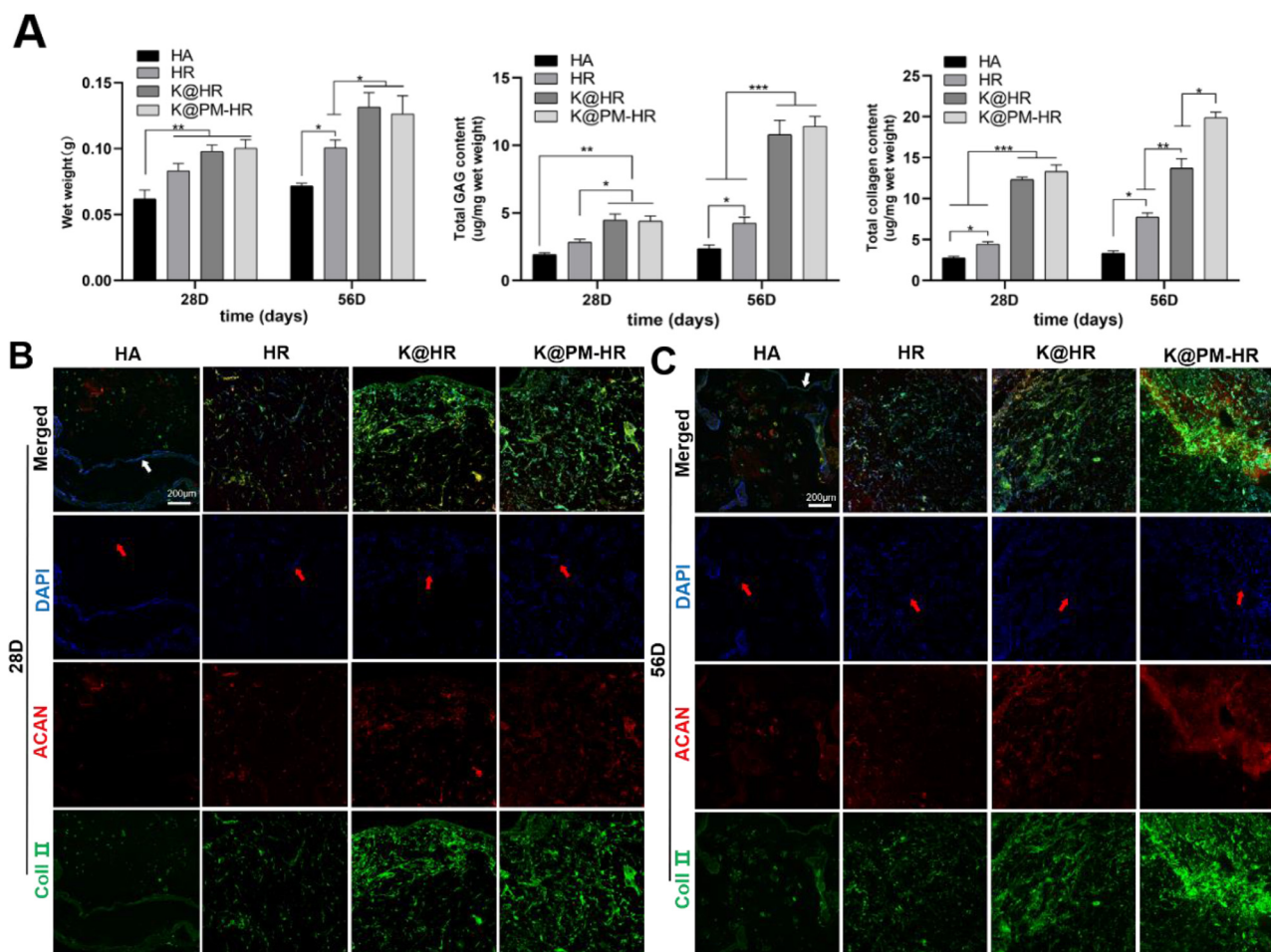
Fig. 8. Chondrogenesis of hMSC-laden hydrogel implants after subcutaneous implantation in nude mice. (A) Quantitative analysis of hydrogel weight, collagen, and GAG content 28 and 56 days after subcutaneous implantation. (B) Immunofluorescence staining for chondrogenic-related proteins 28 days after subcutaneous implantation (white arrows: fibrocystic layers; red arrows: cell nucleus). (C) Immunofluorescence staining for chondrogenic-related proteins 56 days after subcutaneous implantation (white arrows: fibrocystic layers; red arrows: cell nucleus). Data are shown as mean ± SD; $n = 3$. * < 0.05, ** < 0.01, *** < 0.001. (For interpretation of the references to colour in this figure legend, the reader is referred to the web version of this article.)

4. Conclusion

In this study, the system of K@PM-HR hydrogel successfully furnish a cell microenvironment to facilitate stem cell differentiation during neochondrogenesis. The RGD peptide enhanced cell-matrix interactions and promoted cell survival and proliferation, while the HAV peptide regulated cell-cell interactions. The original intention of the experiment was to use these peptides with various functions to guide different behaviors of cells. However, it was found that, although HAV peptides were not added in early stages of the experiment, the weak cross-linked gel matrix enhanced cell proliferation and even agglutination under the action of RGD peptide. Of course, with the participation of HAV and RGD, the cells exhibited more obvious aggregation and chondrogenesis due to the actions of these two peptides. As a key step in regulating cell differentiation, sustainable release of KGN promoted chondrogenic differentiation of hMSCs. Therefore, this functionalized HA hydrogel has promise as a stem cell culture system and scaffold matrix for clinical applications, including 3D-printed gel scaffolds, microfluidic technologies, and cartilage tissue engineering.

Declaration of Competing Interest

All authors have read and approved the final version of the submitted manuscript. We declare no conflicts of interest in this work.

Acknowledgments

Supplementary materials

Supplementary material associated with this article can be found, in the online version, at doi:10.1016/j.actbio.2020.12.054.

Reference

[1] T.M. Simon, D.W. Jackson, Articular cartilage: injury pathways and treatment options, Sports Med. Arthrosc. 14 (3) (2006) 146–154.

[2] Y. Wu, S. Zhu, C. Wu, C. Lu, C. Hu, S. Xiong, J. Chang, B.C. Heng, Y. Xiao, H.W. Ouyang, A bi-lineage conducive scaffold for osteochondral defect regeneration, Adv. Funct. Mater. 24 (28) (2014) 4473–4483.

[3] E.B. Hunziker, Articular cartilage repair: are the intrinsic biological constraints undermining this process insuperable? Osteoarthr. Cartil. 7 (1) (1999) 15–28.

[4] D.J. Huey, J.C. Hu, K.A. Athanasiou, Unlike bone, cartilage regeneration remains elusive, Science (New York, N.Y.) 338 (6109) (2012) 917–921.

[5] T.M. Acri, K. Shin, D. Seol, N.Z. Laird, I. Song, S.M. Geary, J.L. Chakka, J.A. Martin, A.K. Salem, Tissue Engineering for the Temporomandibular Joint, Adv. Healthc. Mater. 8 (2) (2019) e1801236.

[6] M. Bhattacharjee, J. Coburn, M. Centola, S. Murab, A. Barbero, D.L. Kaplan, I. Martin, S. Ghosh, Tissue engineering strategies to study cartilage development, degeneration and regeneration, Adv. Drug Deliv. Rev. 84 (2015) 107–122.

[7] I.L. Kim, R.L. Mauck, J.A. Burdick, Hydrogel design for cartilage tissue engineering: a case study with hyaluronic acid, Biomaterials 32 (34) (2011) 8771–8782.

[8] S.J. Bidarra, C.C. Barrias, P.L. Granja, Injectable alginate hydrogels for cell delivery in tissue engineering, Acta Biomater. 10 (4) (2014) 1646–1662.

[9] Z. Shariatinia, A.M. Jalali, Chitosan-based hydrogels: preparation, properties and applications, Int. J. Biol. Macromol. 115 (2018) 194–220.

[10] L.H. Chen, J.F. Xue, Z.Y. Zheng, M. Shuhaidi, H.E. Thu, Z. Hussain, Hyaluronic acid, an efficient biomacromolecule for treatment of inflammatory skin and joint diseases: a review of recent developments and critical appraisal of preclinical and clinical investigations, Int. J. Biol. Macromol. 116 (2018) 572–584.

[11] G.D. Prestwich, Hyaluronic acid-based clinical biomaterials derived for cell and molecule delivery in regenerative medicine, J. Control. Release 155 (2) (2011) 193–199.

[12] J. Lam, N.F. Truong, T. Segura, Design of cell-matrix interactions in hyaluronic acid hydrogel scaffolds, Acta Biomater. 10 (4) (2014) 1571–1580.

[13] Q. Feng, M. Zhu, K. Wei, L. Bian, Cell-mediated degradation regulates human mesenchymal stem cell chondrogenesis and hypertrophy in MMP-sensitive hyaluronic acid hydrogels, PLoS ONE 9 (6) (2014) e99587.

[14] H. An, J.W. Lee, H.J. Lee, Y. Seo, H. Park, K.Y. Lee, Hyaluronate-alginate hybrid hydrogels modified with biomimetic peptides for controlling the chondrocyte phenotype, Carbohydr. Polym. 197 (2018) 422–430.

[15] I.G. Kim, J. Ko, H.R. Lee, S.H. Do, K. Park, Mesenchymal cells condensation-inducible mesh scaffolds for cartilage tissue engineering, Biomaterials 85 (2016) 18–29.

[16] E. Ruoslahti, RGD and other recognition sequences for integrins, Annu. Rev. Cell Dev. Biol. 12 (1996) 697–715.

[17] U. Hersel, C. Dahmen, H. Kessler, RGD modified polymers: biomaterials for stimulated cell adhesion and beyond, Biomaterials 24 (24) (2003) 4385–4415.

[18] Y. Lei, S. Gojgini, J. Lam, T. Segura, The spreading, migration and proliferation of mouse mesenchymal stem cells cultured inside hyaluronic acid hydrogels, Biomaterials 32 (1) (2011) 39–47.

[19] J. Lam, T. Segura, The modulation of MSC integrin expression by RGD presentation, Biomaterials 34 (16) (2013) 3938–3947.

[20] N. Huebsch, P.R. Arany, A.S. Mao, D. Shvartsman, O.A. Ali, S.A. Bencherif, J. Rivera-Feliciano, D.J. Mooney, Harnessing traction-mediated manipulation of the cell/matrix interface to control stem-cell fate, Nat. Mater. 9 (6) (2010) 518–526.

[21] O. Chaudhuri, L. Gu, D. Klumpers, M. Darnell, S.A. Bencherif, J.C. Weaver, N. Huebsch, H.P. Lee, E. Lippens, G.N. Duda, D.J. Mooney, Hydrogels with tunable stress relaxation regulate stem cell fate and activity, Nat. Mater. 15 (3) (2016) 326–334.

[22] L. Bian, C. Hou, E. Tous, R. Rai, R.L. Mauck, J.A. Burdick, The influence of hyaluronic acid hydrogel crosslinking density and macromolecular diffusivity on human MSC chondrogenesis and hypertrophy, Biomaterials 34 (2) (2013) 413–421.

[23] H.P. Lee, L. Gu, D.J. Mooney, M.E. Levenston, O. Chaudhuri, Mechanical confinement regulates cartilage matrix formation by chondrocytes, Nat. Mater. 16 (12) (2017) 1243–1251.

[24] A.M. DeLise, L. Fischer, R.S. Tuan, Cellular interactions and signaling in cartilage development, Osteoarthr. Cartil. 8 (5) (2000) 309–334.

[25] B.K. Hall, T. Miyake, All for one and one for all: condensations and the initiation of skeletal development, BioEssays 22 (2) (2000) 138–147.

[26] O.W. Blaschuk, R. Sullivan, S. David, Y. Pouliot, Identification of a cadherin cell adhesion recognition sequence, Dev. Biol. 139 (1) (1990) 227–229.

[27] L. Bian, M. Guvendiren, R.L. Mauck, J.A. Burdick, Hydrogels that mimic developmentally relevant matrix and N-cadherin interactions enhance MSC chondrogenesis, Proc. Natl. Acad. Sci. U.S.A. 110 (25) (2013) 10117–10122.

[28] M.Y. Kwon, S.L. Vega, W.M. Gramlich, M. Kim, R.L. Mauck, J.A. Burdick, Dose and timing of N-cadherin mimetic peptides regulate MSC chondrogenesis within hydrogels, Adv Healthc Mater 7 (9) (2018) e1701199.

[29] I.L. Kim, S. Khetan, B.M. Baker, C.S. Chen, J.A. Burdick, Fibrous hyaluronic acid hydrogels that direct MSC chondrogenesis through mechanical and adhesive cues, Biomaterials 34 (22) (2013) 5571–5580.

[30] K. Johnson, S. Zhu, M.S. Tremblay, J.N. Payette, J. Wang, L.C. Bouchez, S. Meeusen, A. Althage, C.Y. Cho, X. Wu, P.G. Schultz, A stem cell-based approach to cartilage repair, Science (New York, N.Y.) 336 (6082) (2012) 717–721.

[31] J. Zhang, J.H. Wang, Kartogenin induces cartilage-like tissue formation in tendon-bone junction, Bone Res 2 (2014) 14008.

[32] M.L. Kang, J.Y. Ko, J.E. Kim, G.I. Im, Intra-articular delivery of kartogenin-conjugated chitosan nano/microparticles for cartilage regeneration, Biomaterials 35 (37) (2014) 9984–9994.

[33] J. Xu, Q. Feng, S. Lin, W. Yuan, R. Li, J. Li, K. Wei, X. Chen, K. Zhang, Y. Yang, T. Wu, B. Wang, M. Zhu, R. Guo, G. Li, L. Bian, Injectable stem cell-laden supramolecular hydrogels enhance *in situ* osteochondral regeneration via the sustained co-delivery of hydrophilic and hydrophobic chondrogenic molecules, Biomaterials 210 (2019) 51–61.

[34] T.P. Richardson, M.C. Peters, A.B. Ennett, D.J. Mooney, Polymeric system for dual growth factor delivery, Nat. Biotechnol. 19 (11) (2001) 1029–1034.

[35] D.S. Benoit, S.D. Collins, K.S. Anseth, Multifunctional hydrogels that promote osteogenic hMSC differentiation through stimulation and sequestering of BMP2, Adv. Funct. Mater. 17 (13) (2007) 2085–2093.

[36] Q. Yang, B.H. Teng, L.N. Wang, K. Li, C. Xu, X.L. Ma, Y. Zhang, D.L. Kong, L.Y. Wang, Y.H. Zhao, Silk fibroin/cartilage extracellular matrix scaffolds with sequential delivery of TGF-β3 for chondrogenic differentiation of adipose-derived stem cells, Int. J. Nanomedicine 12 (2017) 6721–6733.

[37] Z. Luo, S. Zhang, J. Pan, R. Shi, H. Liu, Y. Lyu, X. Han, Y. Li, Y. Yang, Z. Xu, Y. Sui, E. Luo, Y. Zhang, S. Wei, Time-responsive osteogenic niche of stem cells: a sequentially triggered, dual-peptide loaded, alginate hybrid system for promoting cell activity and osteo-differentiation, Biomaterials 163 (2018) 25–42.

[38] D. Shi, X. Xu, Y. Ye, K. Song, Y. Cheng, J. Di, Q. Hu, J. Li, H. Ju, Q. Jiang, Z. Gu, Photo-cross-linked scaffold with kartogenin-encapsulated nanoparticles for cartilage regeneration, ACS Nano 10 (1) (2016) 1292–1299.

[39] E.C. Jensen, Quantitative analysis of histological staining and fluorescence using ImageJ, Anat. Rec. (Hoboken, N.J. 296 (3) (2013) 378–381 2007.

[40] J. Yang, Y.S. Zhang, K. Yue, A. Khademhosseini, Cell-laden hydrogels for osteochondral and cartilage tissue engineering, Acta Biomater. 57 (2017) 1–25.

[41] E.A. Aisenbrey, S.J. Bryant, A MMP7-sensitive photoclickable biomimetic hydrogel for MSC encapsulation towards engineering human cartilage, J. Biomed. Mater. Res. A 106 (8) (2018) 2344–2355.

[42] X. Li, J. Ding, Z. Zhang, M. Yang, J. Yu, J. Wang, F. Chang, X. Chen, Kartogenin-incorporated thermogel supports stem cells for significant cartilage regeneration, ACS Appl. Mater. Interfaces 8 (8) (2016) 5148–5159.

[43] M. Zhu, S. Lin, Y. Sun, Q. Feng, G. Li, L. Bian, Hydrogels functionalized with N-cadherin mimetic peptide enhance osteogenesis of hMSCs by emulating the osteogenic niche, Biomaterials 77 (2016) 44–52.

[44] N. Annabi, J.W. Nichol, X. Zhong, C. Ji, S. Koshy, A. Khademhosseini, F. Dehghani, Controlling the porosity and microarchitecture of hydrogels for tissue engineering, Tissue Eng. Part B Rev. 16 (4) (2010) 371–383.

[45] Y.H. Tsou, J. Khoneisser, P.C. Huang, X. Xu, Hydrogel as a bioactive material to regulate stem cell fate, Bioact. Mater. 1 (1) (2016) 39–55.

[46] J. Zhang, A. Mujeeb, Y. Du, J. Lin, Z. Ge, Probing cell-matrix interactions in RGD-decorated macroporous poly (ethylene glycol) hydrogels for 3D chondrocyte culture, Biomed. Mater. (Bristol, England) 10 (3) (2015) 035016.

[47] Y. Tang, S. Lin, S. Yin, F. Jiang, M. Zhou, G. Yang, N. Sun, W. Zhang, X. Jiang, situ gas foaming based on magnesium particle degradation: a novel approach to fabricate injectable macroporous hydrogels, Biomaterials 232 (2020) 119727.

[48] G.C. Yeo, A.S. Weiss, Soluble matrix protein is a potent modulator of mesenchymal stem cell performance, in: Proceedings of the National Academy of Sciences of the United States of America, 116, 2019, pp. 2042–2051.

[49] H.J. Kong, T. Boontheekul, D.J. Mooney, Quantifying the relation between adhesion ligand-receptor bond formation and cell phenotype, in: Proceedings of the National Academy of Sciences of the United States of America, 103, 2006, pp. 18534–18539.

[50] A.T. Metters, K.S. Anseth, C.N. Bowman, Fundamental studies of biodegradable hydrogels as cartilage replacement materials, Biomed. Sci. Instrum. 35 (1999) 33–38.

[51] S. Khetan, M. Guvendiren, W.R. Legant, D.M. Cohen, C.S. Chen, J.A. Burdick, Degradation-mediated cellular traction directs stem cell fate in covalently crosslinked three-dimensional hydrogels, Nat. Mater. 12 (5) (2013) 458–465.

[52] L.J. Green, A.P. Mould, M.J. Humphries, The integrin beta subunit, Int. J. Biochem. Cell Biol. 30 (2) (1998) 179–184.

[53] Y. Takada, X. Ye, S. Simon, The integrins, Genome Biol. 8 (5) (2007) 215.

[54] W. Shi, M. Sun, X. Hu, B. Ren, J. Cheng, C. Li, X. Duan, X. Fu, J. Zhang, H. Chen, Y. Ao, Structurally and Functionally Optimized Silk-Fibroin-Gelatin Scaffold Using 3D Printing to Repair Cartilage Injury In Vitro and In Vivo, Adv. Mater. (Deerfield Beach, Fla.) 29 (29) (2017).

[55] S.A. Oberlender, R.S. Tuan, Expression and functional involvement of N-cadherin in embryonic limb chondrogenesis, Development (Cambridge, England) 120 (1) (1994) 177–187.

[56] E.J. Jin, K.S. Park, D. Kim, Y.S. Lee, J.K. Sonn, J.C. Jung, O.S. Bang, S.S. Kang, TGF-beta3 inhibits chondrogenesis by suppressing precartilage condensation through stimulation of N-cadherin shedding and reduction of cRREB-1 expression, Mol. Cells 29 (4) (2010) 425–432.

[57] J.D. San Antonio, R.S. Tuan, Chondrogenesis of limb bud mesenchyme in vitro: stimulation by cations, Dev. Biol. 115 (2) (1986) 313–324.

[58] A.M. DeLise, R.S. Tuan, Alterations in the spatiotemporal expression pattern and function of N-cadherin inhibit cellular condensation and chondrogenesis of limb mesenchymal cells *in vitro*, J. Cell. Biochem. 87 (3) (2002) 342–359.

[59] T.A. Petrie, J.E. Raynor, D.W. Dumbauld, T.T. Lee, S. Jagtap, K.L. Templeman, D.M. Collard, A.J. García, Multivalent integrin-specific ligands enhance tissue healing and biomaterial integration, Sci. Transl. Med. 2 (45) (2010) 45ra60.

[60] Q. Ji, Y. Zheng, G. Zhang, Y. Hu, X. Fan, Y. Hou, L. Wen, L. Li, Y. Xu, Y. Wang, F. Tang, Single-cell RNA-seq analysis reveals the progression of human osteoarthritis, Ann. Rheum. Dis. 78 (1) (2019) 100–110.

[61] Y. Zhu, J. Tan, H. Zhu, G. Lin, F. Yin, L. Wang, K. Song, Y. Wang, G. Zhou, W. Yi, Development of kartogenin-conjugated chitosan-hyaluronic acid hydrogel for nucleus pulposus regeneration, Biomater. Sci. 5 (4) (2017) 784–791.

[62] Z. Jia, S. Wang, Y. Liang, Q. Liu, Combination of kartogenin and transforming growth factor-β3 supports synovial fluid-derived mesenchymal stem cell-based cartilage regeneration, Am. J. Transl. Res. 11 (4) (2019) 2056–2069.

[63] Y. Zhao, B. Teng, X. Sun, Y. Dong, S. Wang, Y. Hu, Z. Wang, X. Ma, Q. Yang, Synergistic effects of kartogenin and transforming growth factor-β3 on chondrogenesis of human umbilical cord mesenchymal stem cells in vitro, Orthop. Surg. 12 (3) (2020) 938–945.

[64] J. Yang, Y. Liu, L. He, Q. Wang, L. Wang, T. Yuan, Y. Xiao, Y. Fan, X. Zhang, Icariin conjugated hyaluronic acid/collagen hydrogel for osteochondral interface restoration, Acta Biomater. 74 (2018) 156–167.

[65] E.M. Thompson, A. Matsiko, E. Farrell, D.J. Kelly, F.J. O'Brien, Recapitulating endochondral ossification: a promising route to *in vivo* bone regeneration, J. Tissue. Eng. Regen. Med. 9 (8) (2015) 889–902.

[66] A. Petersen, A. Princ, G. Korus, A. Ellinghaus, H. Leemhuis, A. Herrera, A. Klaumünzer, S. Schreivogel, A. Woloszyk, K. Schmidt-Bleek, S. Geissler, I. Heschel, G.N. Duda, A biomaterial with a channel-like pore architecture induces endochondral healing of bone defects, Nat. Commun. 9 (1) (2018) 4430.

[67] F. Long, D.M. Ornitz, Development of the endochondral skeleton, Cold. Spring. Harb. Perspect. Biol. 5 (1) (2013) a008334.

[68] J.A. Panadero, S. Lanceros-Mendez, J.L. Ribelles, Differentiation of mesenchymal stem cells for cartilage tissue engineering: individual and synergetic effects of three-dimensional environment and mechanical loading, Acta Biomater. 33 (2016) 1–12.

[69] J.M. Anderson, A. Rodriguez, D.T. Chang, Foreign body reaction to biomaterials, Semin. Immunol. 20 (2) (2008) 86–100.

[70] L. Bian, D.Y. Zhai, E. Tous, R. Rai, R.L. Mauck, J.A. Burdick, Enhanced MSC chondrogenesis following delivery of TGF-β3 from alginate microspheres within hyaluronic acid hydrogels *in vitro* and *in vivo*, Biomaterials 32 (27) (2011) 6425–6434.